Transactions of the Korean Society of Mechanical Engineers Vol. 1, No. 1, pp. 17~25, 1977

<Original>

Effect of Wall Proximity on Air Bubbles Rising in Liquid

Joon Mo Kang*

(Received 1976. 10. 14)

액체중을 상승하는 공기포의 관벽영향

姜 準 模

요 약

관벽의 영향을 무시할 수 있는 용기내의 액체중을 상승하는 단일공기포의 상승속도, 형상, 경로를 명확히하고 원주형관, 정방형관, 평행평판간의 액체중을 상승하는 단일기포의 상승속도에 미치는 관벽영향을 구하였다. 원주형관을 상승하는 공기포는 dimensionless plot로 실험치를 통일적으로 표현할 수가 있었으며 관벽영향을 받지않고 관중을 상승할 수 있는 공기포에 대한 최저의 관경을 결정할 수가 있었다.

Abstract

The purpose of this paper is to clarify the effect of wall proximity on the terminal velocity of single air bubbles in vertical tubes. As an initial step, experiments were conducted to determine the terminal velocity, shape, and path of single air bubbles rising freely in water.

The terminal velocity of air bubbles rising through water was measured in cylindrical tubes, rectangular tubes, and parallel plates respectively.

The results of effect wall of cylindrical tubes were shown as a dimensionless plot, and may also be used to arrive at a decision regarding the minimum size of tube.

1. Introduction

Air bubbles are formed in water naturally or artificially. As in water turbine or a pump, atmospheric air naturally mixed with water expands to form large bubbles in the space where the pressure is very low, in the draught or suction tube, which destory the effective action of the machine.

The results of many experimenters[1-6] on the terminal velocity of gas bubbles moving in stationary liquid field have been published. These results show considerable scatter and uncertainty. Therefore, some tests were repeated in order to determine the rate of air bubbles in water. Except for a few investigations, the data were taken in tanks or tubes the walls of which were sufficiently close to the moving bubble to cause some

* Member, Association of Asia Technical Cooperation.

Discussion on this paper should be addressed to the Editorial Department, KSME, and will be accepted until June 15, 1977.

doubt as to the absence of boundary effects. The problem of effect of the walls of the tube on the velocity of rise of the bubble attracts considerable.

The experiments described in this report consisted of the determination of the terminal velocity, shape, and path of single air bubbles rising freely in water of the large tank. The effect of the walls of the vertical tube on the velocity of rise of the bubble was also investigated. The results may also be used to arrive at a decision regarding the minimum size of tube or tank in which experimental data may be taken from the movement of single bubbles if wall effects are to be avoided or are to be held below some predetermined value.

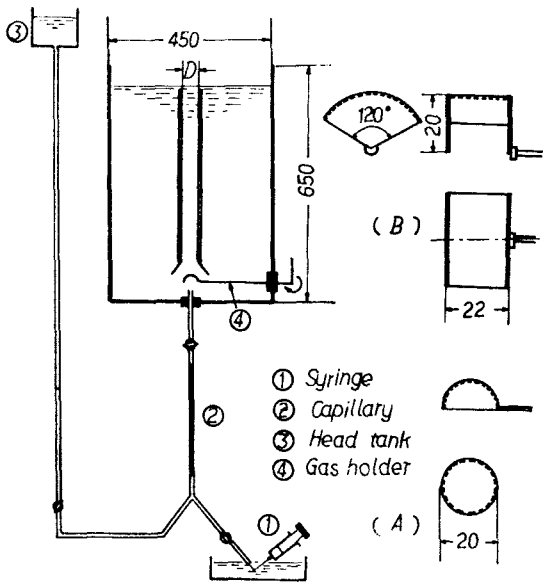

Fig. 1. Skematic diagram of experimental apparatus

2. Test Apparatus

The test performed in the transparant-wall tank, which is large tank enough to preclude wall effect and to insure a minimum of turbulence effects. A sketch of the apparatus is shown in Fig. 1. A 35×45×65cm tank, having 0.4cm-thick glass walls, was used to contain the tap water. Most of the tests were run at a water temprature of 22°C. The test procedure using the tip of a glass tube to form air bubbles was as follow: Air was injected from a graduated syringe in to a capillary tube with known diameter. Then the total volume of air contained in the capillary was measured. After measurement, the air was transferred from the capillary tube to the gas holder by the hydrostatic head of a reservoir of water located 50cm above the tank. The gas holder was then rotated to discharge a single bubble in the liquid. The shape of the gas holder is illustrated in Fig. 1 [A, B]. This design allows one to reduce asymmetrical release impulses given to the bubble and stable single bubbles without stallites were readily obtained in this manner.

The illumination necessary for the photographs was obtained by a stroboscopic lamp located over the surface of the water in the tank which in turn was powered by a stroboscope which has a frequency of about 30 cycles/sec. The room was darkened during the tests. A vertical scale and a plumb line within the field of view of the camera is used in determining the position of bubble during its ascent. The time during ascent was determined from the knowledge of the frequency of the stroboscope.

The observation of the effect of wall proximity were made in six cylindrical tubes of 4.0, 2.5, 1.55, 1.03, 0.85, 0.64cm and seven rectangular tubes of 6×6, 4×4, 3×3, 2×2, 1.5×1.5, 1×1, 0.5×0.5cm, and seven

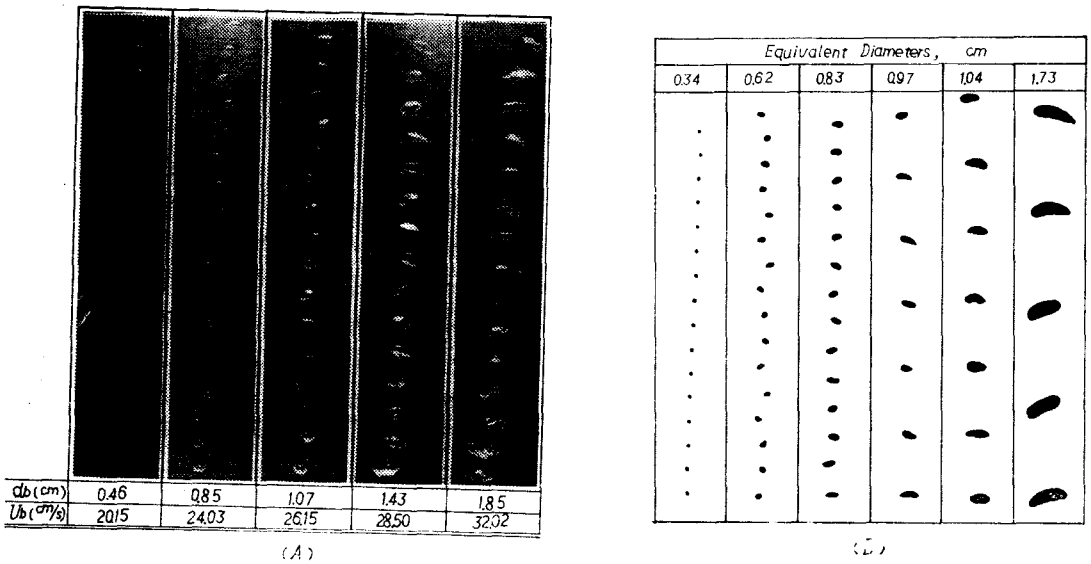

Fig. 2. Photographs showing the shape and paths of typical bubbles

parallel plates of 6, 4, 2.5, 2, 1.5, 1, 0.5 cm. Each was 80cm.

In the case of bubbles, it is most convenient to use a length parameter which is based on its volume rather than a physical dimension as is customary for rigid bodies. The length parameter chosen is the equivalent diameter d_b where

$$d_b = (6/\pi \cdot V_b)^{1/3}$$

3. Results

3.1. Behavior and shape of rising bubbles in quiescent water

By the photographic and observational results, it was found that three general types of shape of the bubble and its resultant behavior in a tank of infinite extent are generally recognized;

1. Small bubbles (<0.2cm). These have a spherical shape and ascend in a straight line.

2. Medium size (0.2 0.6cm). In this region the bubbles are visibly deform; they ascend with a spiral or zigzag movement.

3. Large bubbles (>0.6cm). The bubbles again ascend in a straight line but they are largely deformed and finally they obtain a more or less mushroom-like shape.

It was observed in the experiments that, as the bubbles size was increased, a change in bubble shape from spherical to ellipsoidal to mushroom-like shape occured in water. Very small bubbles are spherical. Large bubbles are flattened, i.e., ellipsoidal in shape, whereas very large bubbles assume a mushroom-like shape. But the transition points at which these shape-change occur are not clear.

Photographs of typical shapes are shown in Fig. 2. It should be noted here that some of the shapes shown in these photographs are instantaneous shapes, since the shape of large bubbles does not remain constant during the ascent.

A description in geometrical terms of the bubble in the various flow regions may be of interest. Since a bubble fluctuates in shape as it rises, all bubble dimensions which were obtained from the photographs represent average values. For the bubbles which can be approximated by oblate ellipsoids, a completely descriptive shape parameter is the ratio of the major to minor axes b/a. This is shown as a function of bubble size in Fig. 3 using data obtained for typical bubbles. As the equivalent diameter increase, the bubbles becomes flatter until a maximum ratio about 0.3 is reached at an equivalent diameter of about 1.2cm. Beyond this size, the ratio remains the same but the shape of the bubble becomes increasing irregular. Finally, at a value d_b greater than 1.6cm, the shape varies so greatly, as the bubble size, that no specific values of b/a can be assigned. The transition to mushroomlike shape is completed at an equivalent diameter of 2cm.

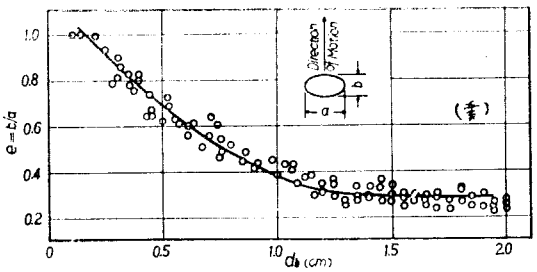

Fig. 3. Effect of bubble size on the shape of ellipsoidal air bubbles rising in water

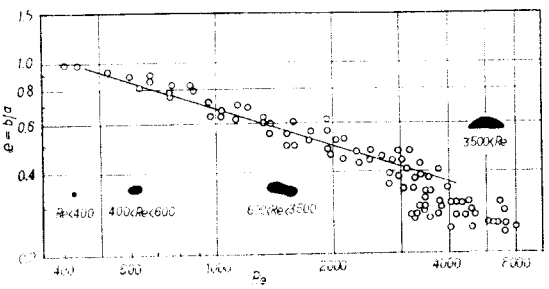

Fig. 4. Effect of Reynolds number on the shape of ellipsoidal air bubbles

Fig. 4 shows the ratio of b/a curve of the bubbles in terms of Reynolds numbers. The typical bubble shape of the regions of Reynolds number is indicated in this figure. It will be observed that, in region of Re<400, the bubbles have a spherical shape, and 400 <Re<3500, deformed bubbles oblate ellipsoidal shape, and at Re<3500, deformed bubbles assuming an irregular mushrocm-like shape.

Since bubbles of different size will assume different shapes, the equivalent diameter d_b, defined as the diameter of a sphere having the same volume as that the bubble, was used as the length parameter. Fig. 5 shows the terminal velocity of air bubbles rising freely in tap water as a function of the equivalent diameter. The data in Fig. 5 represents average values which were obtained from the all photographs. The other data are also included in Fig. 5. This shows clearly that for the ascending of bubbles three regions can be distinguished.

1. Small bubbles (<0.2cm). The terminal velocity increases with increasing bubble

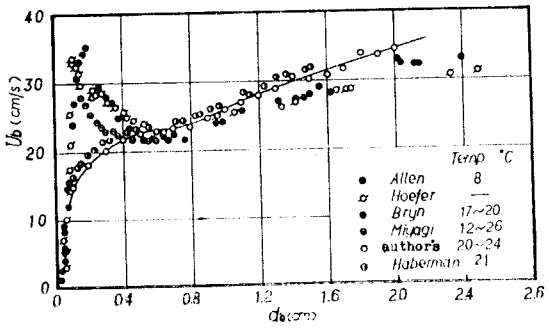

Fig. 5. The terminal velocity of air bubbles in water as a function of bubble size

diameter.

2. Medium-size bubbles (0.2-0.6cm). The irregular character of movement causes spreading of the data.

3. Large bubbles (>0.6cm). Bubble velocity increases slightly with increasing diameter.

In the second region, the spreading of data will doubtless depend on physical properties of the liquid(viscosity and surface tension). There is need for more experimental data in this field.

Stokes contributed to the knowledge on the general problem of fluid flow past bodies in the stream by solving the equation of viscous motion for the case of a rigid spherical particle immersed in a fluid of infinite extend. The main result of this analysis, an expression for the terminal or steady-state velocity of a particle, is known as Stokes' law. When applied to the rise of a gas bubble in a liquid, Stokes' law gives

$$U_\infty = \frac{g(\rho_1-\rho_2)d_b^2}{18\mu} \qquad (1)$$

where U_∞ is steady-state, terminal rising velocity, g is gravitational acceleration, ρ_1 is liquid density, ρ_2 is gas density, d_b is equivalent diameter, μ is liquid viscosity.

Agreement of Equation (1) with experiment depends on the degree to which the assumptions underlying Stokes law can be satisfied, i.e., spherical rigid particle with no slip at the particle boundary, inertia forces small magnitude compared to viscous forces, gravity the only extraneous force, and constant fluid properties. The inability to solve hydrodynamic equations of motion for systems where Stokes' law does not apply has lead to the practice of employing an arbitrarily defined drag coefficient to summarize experimental data. The drag coefficient is usually defined by the equation

$$C_D = \frac{\text{Drag force}}{\frac{1}{2}\rho_1 U_b^2 A} \qquad (2)$$

where C_D is the drag coefficient, and A is the projected area. For convencience, A can be redefined to be the projected area of a sphere of equal volume. In addition, the drag force for a bubble at its terminal velocity is equal to the bouyant force $V_b\rho g$ where V_b is volume of the bubble. Hence, in terms of the equivalent diameter, the expression for the drag coefficient reduces to

$$C_D = \frac{4}{3} g \frac{d_b}{U_b^2} \qquad (3)$$

Figure 6 shows the relationship between C_D and Re for all of these experiments on air bubbles in water. The corresponding curve for rigid spheres is also included in Figure 6.

Examination of Figure 6 shows that up to a Reynolds number of 70, the bubble behaves like a rigid sphere. For a Reynolds number range 70 to 400, the bubble, although

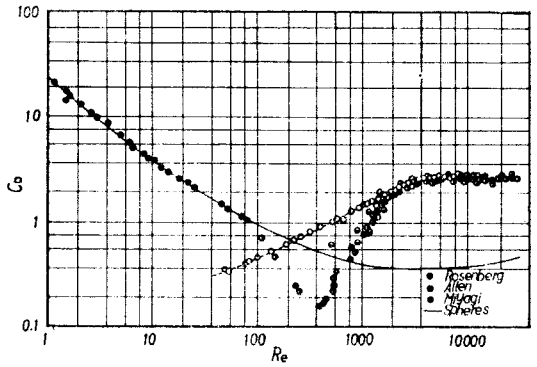

Fig. 6. The drag coefficient as a function of Reynolds number for air bubbles rising at their terminal velocity

still spherical, has a drag coefficient consi derably less than rigid spheres. This may be due to the development of slip at the boundaries[7]. Beyond a Reynolds number of 400, the hydrodynamic and surface tension forces are both important in determining the shape and consequently the drag coefficient of the bubble. As the bubble size increases, the shape of the bubble becomes flatter with a consequent rise in the value of the drag coefficient. For a Reynolds number greater than 5,000, surface tension plays relatively minor role in determining the shape of the bubble; hydrodynamic forces acting on the bubble result in the mushroom-like shape.

The results of the present tests determined a constant drag coeffcient of 2.6 for the mushroom-like bubbles. The velocity of mushroom-like bubbles of given size rising in water can be determined from constant value of the drag coefficient or directly from the velocity curve (Figure 5). For $C_D=(4/3)gd_b/U_b^2=2.6$, we obtain for the rate of rise of the mushroom-like bubbles in water.

$$U_b=0.72\sqrt{gd_b} \qquad (4)$$

Thus, the velocity of rise these bubbles is function of the bubble size only.

3.2 Effect of wall proximity

The effect of tube-wall proximity in the terminal velocity of air bubbles in the cylindrical tubes, rectangular tubes, and parallel plates is shown in Figure 7, 8, and 9.

In Figure 7 and 8, the upper curve is the velocity of air bubbles rising in the large tank (Figure 5). The upper curve is considered to represent the relationship in an infinite medium as the curves for each of the small tubes lead it at some point.

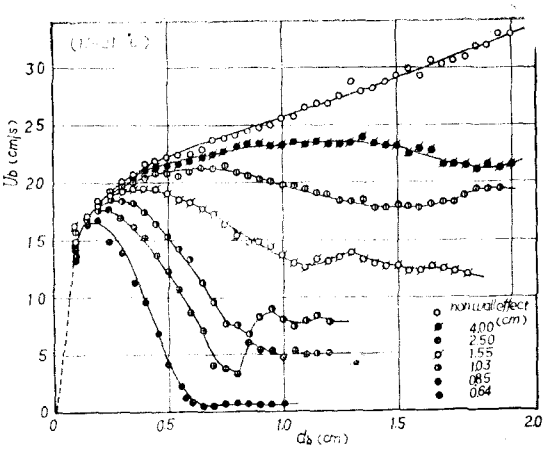

Fig. 7. The terminal velocity of air bubbles in water of cylindrical tubes as a function of bubble size

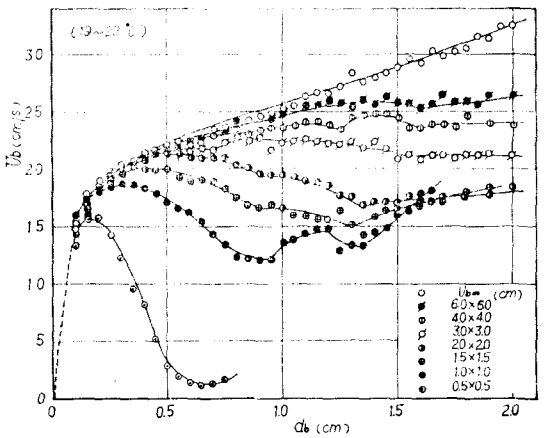

Fig. 8. The terminal velocity of air bubbles in water of rectangular tubes as a function of bubble size

The bubbles ascending in the cylindrical and rectangular tube exhibited three distinct modes of motion, as follows;

I. A spiraling ascent without periodic tipping about horizontal axis.

2. A straight ascent with periodic tipping.

3. A straight ascent without spiraling or tipping.

The peculiar shape of the velocity curve (Figure 7) in the 1.03cm tube is directly attributable to changes in the modes of motion. Up to d_b=0.3cm, the bubbles were slightly flattened but moved without spiraling or tipping. Above this point spiraling developed with increasing period and amplitude up to d_b=0.85cm. Apparently the explanation of this decrease in velocity is that the resistance increases both because of the increased length of actual path and the decreased average distance from the wall. Beyond d_b=0.85cm, tipping developed, but the amplitude and period decreases and had disappeared at d_b=0.95cm. Beyond this value the velocity was practically independent of the size. Tipping did not occur in the 0.64-cm tube, probably because the stabilizing effect of the walls became appreciable before the bubbles had attained a size consistent with this type of motion. Spiraling motion was observed in the large tubes but did not cause rapidly decreasing velocity with increasing size. This circumstance may indicate that the wall effect was the cause of the decrease in the case of the 1.03-cm tube rather than increases in the length of path. In the tubes larger than 1.03-cm spiraling was always present, and it is possible that the velocity curve would have dropped from its maximum value as occured in the smaller tubes, if it had been possible to generate large bubbles. Tipping was not observed in the large tubes, and this may indicate that it results from the dragging effect of the wall.

The velocity curves for the rectangular tubes are similar to those in the cylindrical tubes. The velocity curve in the parallel plates show a steady increase with diameter

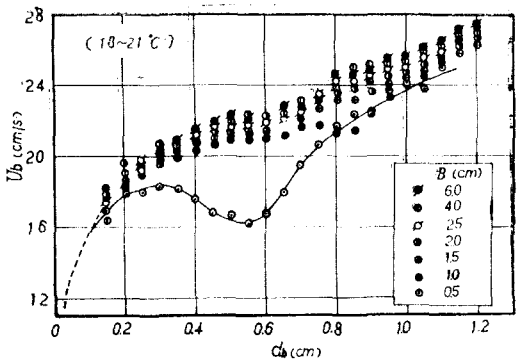

Fig. 9. The terminal velocity of air bubbles in water of parallel plates as a function of bubble size

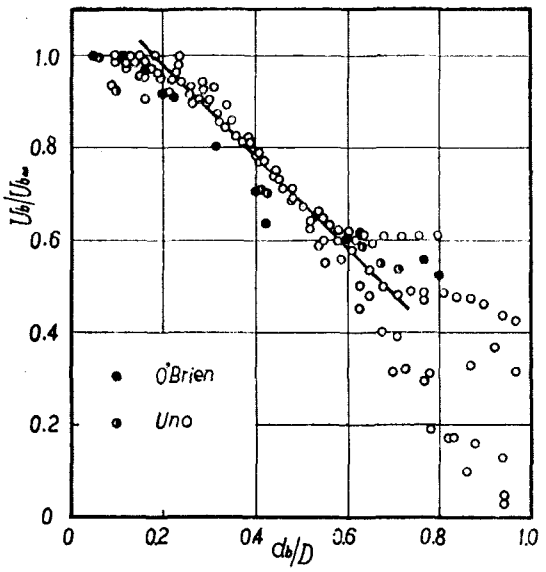

Fig. 10. The variation of rising velocity for ratio of bubble size and cylindrical tube size

which seems to confirm the explanations of the peculiarities in curves for the cylindrical and rectangular tube.

In connection with the velocity diagrams, the use of the diameter of an equivalent sphere as a measure of the size of a bubble makes it possible to have a value of d_b greater than the diameter of the tube.

For the cylindrical tubes, values of $(U_b/U_{b\infty})$ and (d_b/D) were calculated from Figure 7 and plotted as shown in Figure 10. O' Brien's[7] and Uno's[8] data are included for comparison in this Figure.

In Figure 10 the variation of the terminal velocity of air bubbles can be seen with increases d_b/D ratio. It is seen that, up to about $d_b/D \approx 0.6$, the majority of the point lie on the stright line. By the observation on the behavior of bubbles in the proximity of the wall, the bubbles of a stable ellipsoidal form generally rise in a helical path. Large bubbles of unstable shape rise in irregular rocking motion. The horizontal component of the motion cannot exceed the tube diameter and as the helical diameter approaches this value, there is a damping effect on the helical motion. As the diameter of the bubble approaches the tube diameter, the bubble tends to change to the cylindrical form. For mushroom-like shaped bubbles this would occure at a (d_t/D) ratio of about 0.5.

Figure 11 shows the relationship between C_D and R_e for the experimental data of rising air bubbles in the cylindrical tubes. O' Brien's data on air bubbles in three different tubes are compared with the author's results.

Examination of Figure 11 shows that, for a Reynolds number rigion of R_e 200, the bubble has a drag coefficient considerably less than rigid spheres. Beyond a Reynolds number of 200, the drag coefficient increases as Reynolds number was increased, and then breaks away from the curve of an infinite medium abruptly. As the tube diameter becomes smaller, the Reynolds number value of breaking away from the curve of infinite medium becomes also small.

In Figure 11, the both C_D and R_e is included the terminal velocity, U_b. By the general way, we times both side of Equation (3) by R_e^2 to get

$$C_D R_e^2 = (4/3) g d_b^3 \rho_w^2 / \mu^2 \tag{5}$$

We assume that the terminal velocity, U_b is sought the dimensional function in the form.

$$U_b = f_1(d_d, \rho_w, \mu, g, D) \tag{6}$$

By dimensional analysis we can get a solution in the form

$$R_e = f_2\left(\frac{d_b^3 g \rho_w^2}{\mu^2}, \frac{d_b}{D}\right) \tag{7}$$

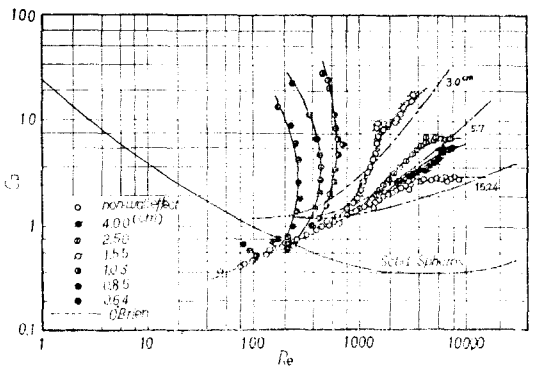

Fig. 11. The drag coefficient as a function of Reynolds number for air bubbles rising in water of cylindrical tubes

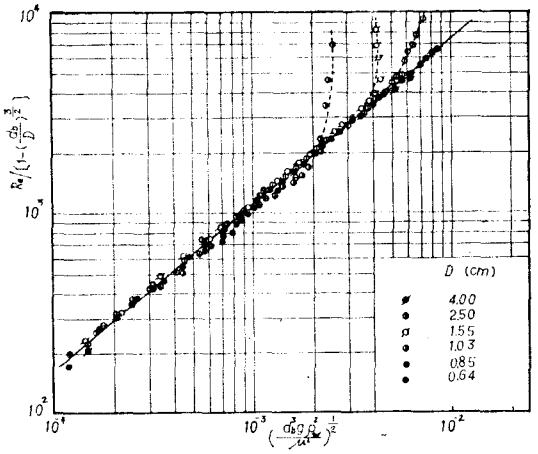

Fig. 12. The dimensionless plot of wall effect on air bubbles rising in cyclindrical tubes

The correction of wall effect was made by $[1-(d_b/D)^{3/2}]$ as was suggested by Munroe[9], and which he based on measurments of the fall of lead shot in water. If we can represent the effect of d_b/D in this equation by the correction factor. Equation (7) becomes

$$\frac{R_e}{\left[1-\left(\frac{d_b}{D}\right)^{3/2}\right]}=f_3\left(\frac{d_b^3 g\rho_w^2}{\mu^2}\right) \qquad (8)$$

Figure 12 shows the results as a dimensionless plot, where the ordinate was Reynolds number corrected by d_b/D and the abscissa was $3C_DR_e^2/4(=d_b^3g\rho_w^2/\mu^2)$. In Figure 12 the straight line is good to determine the velocity of rising bubbles in the cylindrical tube in the rigion $(d_b/D)<0.8$.

Summary

As the size of the bubbles was increased in the tests, there was a change in bubble shape from spherical to ellipsoidal and then to mushroom-like shape in water of the large tank.

Tests on air bubbles at their terminal velocity in water indicate that for Reynolds number of less than 70, bubbles behave like rigid spheres. At greater values of the Reynolds number, the drag coefficients of the bubbles are considerably less than for the rigid spheres even though the bubbles are still spherical in shape. This may be due to the development of slip at the boundaries. For Reynolds numbers from 400 to 5,000 the hydrodynamic and surface-tension forces are both important in determining the shape and consqeuently the drag coeffieient of the bubbles. Beyond this range, hydrodynamic forces almost exclusively determine the shape of the bubble, resulting in a mushroomlike.

The drag coefficients of mushroom-like bubbles are independent of bubble size and have a constant value of 2.6. The rate of rise of these bubbles as a function of the equivalent diameter is given by the experimentally determined relation:

The regarding effect of a near-by cylindrical wall on the terminal velocity of air bubbles rising in the water can be expressed by the straight line in Figure 12 as a dimensionless plot. The minimum size of the tube in which data may be taken if the wall correction is to be negligible is at least ten times the equivalent diameter of the largest bubble to be studied.

Acknowledgment

The work described in this paper was carried out in the Fluid Engineering Laboratory of the Meijii University. The writer wishes to express his indebtedness to Prof. Masato Hirotsu for valuable advice and numerous suggestions.

References

1. H.S. Allen, Phil. Mag., 50, 323 (1900).
2. K. Hoefer, Verein Deutsch. Ing., No. 138, 1 (1913).
3. O. Miyagi, Tech. Reports of Tohcku Imperial University, 5 (1925).
4. T. Bryn, Forsch. Gebiete Ingenieurw., 4, 27 (1933).
5. B. Rosenberg, TMB Report 727, (1950).
6. W.L. Haberman and R.K. Morton, TMB Report 802 (1955).
7. M.P. O'Brien and J.E. Gosline, Ind. Eng. Chem., 27, 1436 (1935).
8. S. Uno and R.C. Kintner, A.I. CH.E. Journal, 2, 420 (1956).
9. H.S. Munroe, Trans. Am. Inst. Min. Eng., 17, 637 (1888).